Radon Monitor using Custom α-detecting MOS IC

R.H. Griffin, H. Le, D.T. Jack, A. Kochermin and N.G. Tarr
Department of Electronics
Carleton University
Ottawa, Ontario Canada K1S 5B6
Email: ngt@doe.carleton.ca

***Abstract*— A passive direct-reading radon monitor utilizing a custom α particle detecting MOS integrated circuit and electrostatic radon progeny concentrator has been designed, built and successfully tested. Radon concentrations at the threshold generally considered hazardous can be detected within hours. This monitor appears suitable for low-cost, high-volume production.**

I. Introduction

Many techniques for radon (^{222}Rn) monitoring are now in use. Silicon diode based detectors are particularly attractive since they offer direct-reading of α emissions produced during radon decay [1]. However, these detectors require expensive large area defect-free diodes, and careful circuit design to avoid noise pick-up and interference. Here, we report a DRAM-inspired α particle detecting integrated circuit we have termed an "αRAM". The αRAM has been incorporated in a fully functional passive radon monitor using electrostatic concentration [2].

II. Background

A. Properties of Radon

Radon is a noble gas produced during the radioactive decay sequence of uranium (^{238}U). Radon decays through a sequence of short lived α emitting progeny with energies in the range of 5 to 8 MeV (Fig. 1). Being chemically inactive and having a half life of nearly 4 days, radon gas produced through uranium decay in the earth's crust can diffuse to the surface where it may become trapped in buildings or enter water supplies [3].

The danger of radon results from α emission during its decay. These particles have little penetration depth and deposit the bulk of their energy in a very short distance. Externally, α radiation poses little danger. The dead layer of skin covering the human body is generally sufficient to absorb all the deposited energy. However, should radon or its progeny be inhaled, sensitive lung tissue is exposed to damaging levels of radiation. There is sufficient energy deposited to either kill or damage live cells. Should these damaged cells reproduce, they may become malignant and induce cancer [4].

Radon decay products tend to be charged. This results in the progeny attaching readily to dust, increasing the likelihood of inhalation. The charged nature of radon progeny can actually be used to advantage to passively concentrate progeny for detection.

Ultimately there is no safe level of exposure to radon gas. However, the U.S. Environmental Protection Agency (EPA) has set a suggested action level of 150 Bq/m^3. Fortunately, it is often quite easy to mitigate the health risks caused by radon. Improved ventilation is often sufficient to reduce radon concentration to levels generally considered safe. There is consequently a need for an inexpensive radon monitor which can be widely deployed.

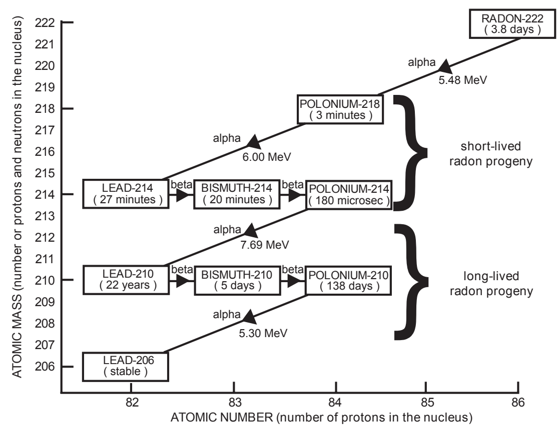

Fig. 1. Radon decay chain

B. Complete Radon Monitoring Systems

Concentration and detection are the two key components of a complete radon monitoring system. As α particles travel only a short distance in air, it is necessary to concentrate the progeny near an α particle detector. There are two classes of concentrators: active and passive.

In active detectors, air is continuously sampled through a filter on which progeny is deposited. A detector located near the filter detects the radioactive decay of the progeny. Active detectors generally read the total activity of all airborne progeny, including that attached to dust. This is typically expressed in "working levels", WL, giving the total potential α particle energy available per liter of air. This type of concentration tends to have a fast response. However, these systems are subject to problems with pump reliability and calibration, and are generally not suitable for extended use with battery power supplies [1].

Passive detectors use electrostatics to concentrate progeny near a detector. Though passive detectors may not offer as fast a response as their active counterparts, their simplicity, cost effectiveness and low power capabilities make them excellent candidates for home radon monitoring.

Passive monitors are often enclosed with a membrane that is permeable to radon gas but not to dust [1]. These monitors typically capture only ^{218}Po. Both the ^{218}Po α emission and subsequent ^{214}Po α emission may be detected. Measurement of the activity of the captured progeny allows direct estimation of the concentration of ^{222}Rn in the air.

There are many different methods for detecting α emissions, ranging from track etch detectors to silicon diode detectors [5]. Simple solutions such as track etch detectors require laboratory analysis for readout, making them inconvenient for home use. Large area silicon diode detectors combined with board-level charge sensitive preamplifiers are direct-reading, but are relatively expensive and prone to noise pickup. The MOS αRAM detector introduced herein can be viewed as a modified diode detector that is direct-reading, noise immune, and very inexpensive to produce in high volume.

III. Monitor Design

A. Interaction of α Particles with Matter

Heavy charged particles, such as α particles, interact with matter primarily through Coulomb forces between their positive charge and the negative charge of the orbital electrons within the absorber material [5]. Paths taken by the α particles tend to be quite straight. Energetic recoiled electrons, referred to as delta rays, are a major contributor to α energy loss. The ultimate result of an α particle passing through an absorber is a dense columnar ionization plasma along the particle's trajectory.

B. Interaction of α Particles with a Silicon pn Junction

An α particle passing through silicon generates one electron-hole pair for every 3.6 eV of energy lost. Thus a typical 6 MeV α particle will produce approximately 2 million electron-hole pairs. In bulk silicon, the electron-hole pairs will eventually recombine. If these pairs are formed in the depletion region of a pn junction, the built-in electric field of the junction will effectively separate them, depositing electrons on the n-type side of the junction and holes on the p-type. The collection efficiency is further enhanced by an effect known as particle induced field funneling [6], in which the dense electron-hole plasma extends the depletion region field deep into the silicon along the track of the α particle (Fig. 2). The end result is that approximately 10^6 electrons cross the depletion region in a typical α interaction.

In silicon diode detectors, the pn junction is usually held in short circuit condition. The charge packet crossing the junction after an α strike is then observed as a current spike in the external circuit, which can be detected with a suitably sensitive amplifier. The approach taken here is to use many small pn junctions, with the n regions precharged to a positive voltage and then allowed to "float" electrically. The injection of electrons into the n-region following an α strike then lowers the voltage across the junction. The advantage of this approach is that the amplifier used to read the voltage change can be monolithically integrated with the pn junction, reducing noise pick-up. In a sophisticated system, it would also be possible to identify defective junctions and eliminate their outputs from consideration, whereas in a traditional diode detector, a single defect renders the whole diode useless.

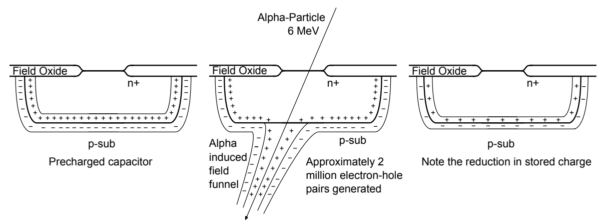

Fig. 2. α particle effect on a precharged pn junction capacitor

To a good approximation, a pn junction formed by an n+ diffusion into a p-type substrate, has a capacitance associated with the depletion region given by

$$C = \frac{\epsilon_S A}{\sqrt{\frac{2\epsilon_S}{q}(\frac{1}{N_A})(\phi_{bi} + V_R)}} \tag{1}$$

using the variable naming conventions of [7].

The voltage change across the junction resulting from injection of a charge pulse Q in response to an α strike is then given by

$$\Delta V = \frac{Q}{C} \tag{2}$$

C. The αRAM

The heart of the αRAM is an array of 100 μm square pn junction capacitor sense cells which are precharged to slightly below the positive supply rail voltage. The sense cell is analogous to the storage capacitor in an early DRAM. For the substrate doping N_A used here, (1) and (2) predict that the cell voltage will be lowered by approximately 0.2 V in response to the million electron charge transfer expected following an α strike. To detect this voltage drop, each sense cell is connected to one input of a conventional cross-coupled latch sense amplifier through an access transistor and bitline. The second input of the sense amplifier is connected through an identical bitline and access transistor to a reference cell identical to the sense cell. A single reference cell is shared by all sense cells in each row in the array. The reference cell is initially precharged to the same voltage as the sense cell, but then a charge equivalent to 5x10^5 electrons (half that expected from an α strike) is removed from the reference cell. In the absence of an α strike on the sense cell, the sense amplifier will therefore invariably determine that the sense cell is higher in voltage than the reference cell. If the sense amplifier determines the sense cell voltage is lower, an α strike is counted. Charge is removed from the reference cell by connecting it to a small "bleeder" pn junction capacitor through an access transistor. The bleeder capacitor is precharged to an adjustable voltage V_{bleed}. Here the bleeder capacitor size was chosen so that a V_{bleed} value of 2 V corresponds to a charge of 5x10^5 electrons.

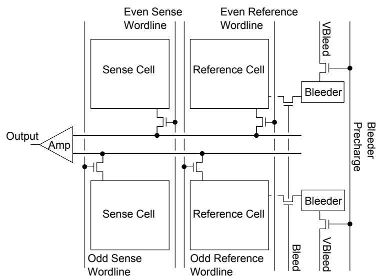

Fig. 3. αRAM folded bitline configuration

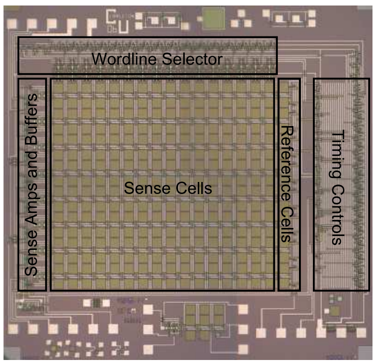

Fig. 4. Fabricated αRAM

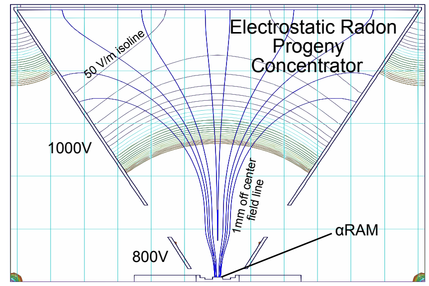

Fig. 5. SATE electrostatic concentrator simulation

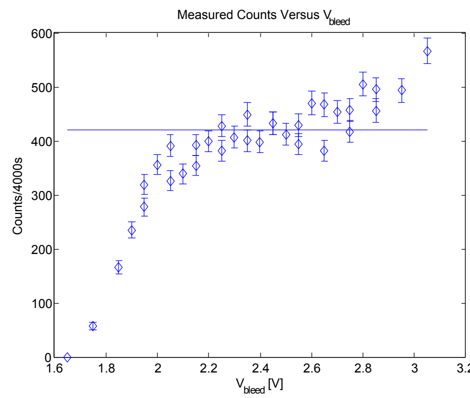

Fig. 6. Quantum efficiency characterization

Each bitline is connected to 16 sense cells and one reference cell in a folded bitline architecture as shown in Fig. 3 [8]. The 3 mm square chip, Fig. 4, includes timing and control logic for refresh and measure states with 16 bitlines. Prototypes were fabricated at Carleton University in a simple nMOS technology.

D. Electrostatic Concentrator

An efficient electrostatic concentrator must deposit progeny from the largest possible volume onto the detector's active area. The electric field inside the swept volume of the concentrator must be large enough that charged progeny have little chance of being neutralized before they are collected. In [2] it was estimated that the residence time due to neutralization is 3 to 6 seconds. The concentrator used here was constructed from a polyethylene funnel of 6 cm radius and 10 cm height with aluminum foil electrodes attached to the funnel interior. Metal mesh, attached to the upper electrode, was placed across the top of the funnel. The design differs from that of [2] in that two electrodes at different potentials were used to establish a stronger sweep field within the funnel. Chip package details necessitated that the detector lie 1 mm below the aperture of the funnel. Electrode size and placement were optimized through extensive simulation with Static Field Analysis Toolkit Educational (SATE) (Fig. 5). With 1000 V applied to the upper electrode and 800 V to the lower, SATE predicts progeny from a swept volume of 70 cm^3 will be deposited on a 1 mm radius target area with a transit time of less than 1 s. The high voltage required by the concentrator was supplied with a 50 stage Cockcroft-Walton charge pump.

IV. Experimental Results

A. Quantum Efficiency

Quantum efficiency measurements were carried out with the αRAM separated by 11 cm from a 33.3 kBq ^{241}Am source in a vacuum chamber at 10 Pa. The device was characterized by varying the amount of charge removed from the reference capacitor. With a small amount of charge removed (higher V_{bleed}) false counts are expected due to the inability of the sense amplifier to recognize small differences in potential. With a large amount of charge removed (low V_{bleed}) the count rate is expected to fall off as only more energetic particles would be detected. With $V_{bleed} \leq 1.6$ V no counts were observed. Fig. 6 shows the experimental results with the expected number of counts, 420, superimposed. The expected number of counts is given by

$$Counts = \frac{SA_{\alpha RAM}}{4\pi r^2_{\alpha Source}} \cdot Activity \cdot Time \qquad (3)$$

where SA is active surface area of the αRAM and $r_{\alpha Source}$ is the distance between the ^{241}Am source and αRAM. Measurements were performed over a period of 4000 s using 48 sense cells.

The αRAM was seen to have a reasonably flat response with V_{bleed} between 2.2 V and 2.8 V. A detection efficiency of $102 \pm 21\%$ is seen over this region. No dark counts were observed when the source was covered by a sheet of paper, confirming that the detector is responding only to α particles, and not the weak γ rays produced in the decay of ^{241}Am.

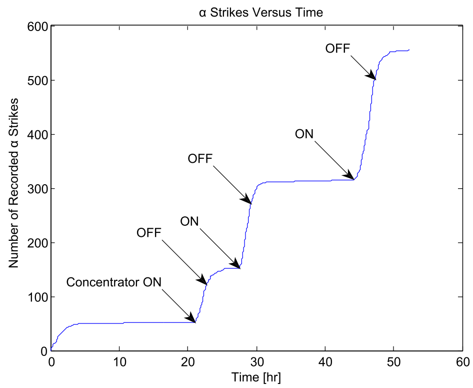

Fig. 7. Typical αRAM and concentrator radon measurement

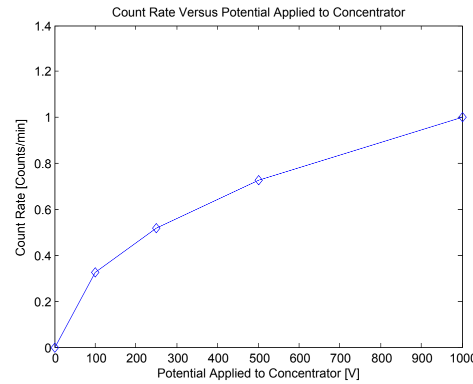

Fig. 8. Electrostatic concentrator collection efficiency

B. Radon Measurement

Measurements were carried out in a sealed 50 liter chamber with radon supplied from crushed rock containing a small amount of uranium. The radon concentration in the chamber was measured with a Ramon 2.2 monitor. The chamber was left undisturbed for one month before measurements were initiated to allow the radon concentration to reach a stable steady-state value and to ensure dust had settled. Fig. 7 shows the results of a typical measurement. Only 8 of 16 bitlines (in the terminology of [8], only odd bitlines) were measured. The count rate is consistent with the expected result given by

$$Rate = P_{event} \cdot Activity_{Chamber} \cdot V_{Conc} \cdot \frac{A_{\alpha RAM}}{A_{Conc}} \quad (4)$$

where P is event probability and includes detection probabilities [9] of both ^{218}Po and ^{214}Po, V is active volume of the concentrator, and A is progeny concentration area and detection area of the αRAM respectively.

With an activity of 2700 Bq/m^3 in the chamber, the count rate was found to be 1.0 counts/min. By extrapolation it would take 30 hours to detect an activity of 150 Bq/m^3 with $\pm 10\%$ accuracy. Using the full array would reduce this time to 15 hours.

It should be noted that when the concentrator voltage is turned off, the detected count rate does not fall immediately to zero, but instead decays exponentially. The time constant for this process is close to the sum of the half-lives for the decay from ^{218}Po to ^{214}Po, as would be expected for progeny decay on the αRAM surface. When the high voltage has been off for an extended period, the background count rate is less than one per hour.

C. Concentrator Characterization

Collection efficiency of the electrostatic concentrator is a function of applied potential. Large potentials should result in high collection efficiency whereas collection efficiency will be reduced at lower potentials. Fig. 8 shows count rate versus collector potential. In all measurements the upper funnel is biased at $V_{applied}$ and the lower section at $0.8V_{applied}$. Each data point was computed by performing a count rate linear regression once the count rate had reached steady state.

V. Conclusion

A passive direct-reading radon monitor utilizing a custom α particle detecting MOS integrated circuit and electrostatic radon progeny concentrator has been designed, built and successfully tested. αRAM quantum efficiency is unity within experimental error. Radon concentrations of 150 Bq/m^3 can be detected in 30 hours with $\pm 10\%$ accuracy. Redesign of the αRAM in a commercial CMOS technology to reduce power consumption will be carried out in the future. This monitor appears suitable for low-cost, high-volume production.

Acknowledgment

The authors wish to thank A. McCarthy for assistance in simulating the αRAM circuit, C. Adams and R. Vandusen for their expert fabrication of the chips, and S. Demtchenko for wirebonding the devices. The contribution of the many students who designed and tested earlier versions of the αRAM is also gratefully acknowledged.

References

[1] H. Bigu and R. Raz, "Passive radon/thoron personal dosimeter using an electrostatic concentrator and a diffused-junction detector," *Rev. Sci. Instrum.*, vol. 56, pp. 146–153, Jan. 1985.

[2] H. Miyake and K. Oda, "Portable and high-sensitive apparatus for measurement of environmental radon using cr-39 track detector," *Journal of Applied Physics*, vol. 26, no. 4, pp. 607–610, Apr. 1987.

[3] U. S. E. P. A. I. E. Division. (2007) A citizen's guide to radon: The guide to protecting yourself and your family from radon. EPA 402-K-07-009. [Online]. Available: http://www.epa.gov/radon/pdfs/citizensguide.pdf

[4] R. Field *et al.*, "An overview of the north american residential radon and lung cancer case-control studies," *J Toxicol Environ Health A*, no. 69:7, pp. 599–631, Apr. 2006.

[5] G. Knoll, *Radiation Detection and Measurement 2nd Ed.* New York, NY: John Wiley and Sons, 1989.

[6] C. Hsieh, P. Murley, and R. O'Brien, "A field-funneling effect on the collection of alpha-particle-generated carriers in silicon devices," *IEEE Electron Device Letters*, vol. EDL-2, no. 4, pp. 103–105, Apr. 1981.

[7] Y. Tsividis, *Operation and Modeling of The MOS Transistor 2nd Ed.* New York, NY: Oxford University Press, 1999.

[8] B. Keeth and R. Baker, *DRAM Circuit Design - A Tutorial*. Piscataway, NJ: IEEE Press, 1999.

[9] K.-D. Chu and P. Hopke, "Neutralization kinetics for polonium-218," *Environmental Science and Technology*, vol. 2, no. 6, pp. 711–717, 1988.